Japanese Journal of Radiology (2018) 36:511–518
https://doi.org/10.1007/s11604-018-0750-3

ORIGINAL ARTICLE

Segmental analysis of respiratory liver motion in patients with and without a history of abdominal surgery

Yasuhiro Shimizu[1,2] · Shigeyuki Takamatsu[1] · Kazutaka Yamamoto[2] · Yoshikazu Maeda[2] · Makoto Sasaki[2] · Hiroyasu Tamamura[2] · Sayuri Bou[2] · Tomoyasu Kumano[1] · Toshifumi Gabata[1]

Received: 16 March 2018 / Accepted: 4 June 2018 / Published online: 20 June 2018

Abstract

Purpose The purpose of this study was to analyze the respiratory motion of each segment of the liver in patients with or without a history of abdominal surgery using four-dimensional computed tomography.

Materials and methods In total, 57 patients treated for abdominal tumors using proton beam therapy were enrolled. Eighteen patients had a history of abdominal surgery and 39 did not. The positions of clearly demarcated, high-density regions in the liver were measured as evaluation points with which to quantify the motion of each liver segment according to the Couinaud classification.

Results In total, 218 evaluation points were analyzed. Comparison of differences in the motion of individual liver segments showed that among patients without a history of surgery, the maximum was 29.0 (7.2–42.1) mm in S6 and the minimum was 15.1 (10.6–19.3) mm in S4. Among patients with a history of surgery, the maximum was 28.0 (9.0–37.4) mm in S7 and the minimum was 6.3 (4.1–9.3) mm in S3.

Conclusion The distances and directions of respiratory motion differed for each liver segment, and a history of abdominal surgery reduced the respiratory motion of the liver. It is necessary to selectively use the internal margin setting.

Keywords Radiotherapy · Liver · Abdominal surgery · Respiratory motion · 4D-CT

Introduction

Primary liver cancer is the most common malignant tumor worldwide and ranks high as a cause of cancer-related death [1, 2]. The liver is a radiosensitive organ; therefore, external beam radiotherapy (RT) is only used for palliation and in selected patients. Recent advancements in RT techniques such as particle beam therapy and stereotactic body radiotherapy (SBRT) have allowed for great extensions in the application of RT for hepatocellular carcinoma. These highly conformal RT techniques have been delivered safely and effectively in patients with liver cancer [3–6]. Particle beam therapy has the physical

Electronic supplementary material The online version of this article (https://doi.org/10.1007/s11604-018-0750-3) contains supplementary material, which is available to authorized users.

✉ Yasuhiro Shimizu
ys.fproton@gmail.com

Shigeyuki Takamatsu
shigerad@staff.kanazawa-u.ac.jp

Kazutaka Yamamoto
k-yamamoto-7m@pref.fukui.lg.jp

Yoshikazu Maeda
y-maeda-ce@pref.fukui.lg.jp

Makoto Sasaki
m-sasaki-hl@pref.fukui.lg.jp

Hiroyasu Tamamura
h-tamamura-8e@pref.fukui.lg.jp

Sayuri Bou
s-bou-oz@pref.fukui.lg.jp

Tomoyasu Kumano
t.kumano@staff.kanazawa-u.ac.jp

Toshifumi Gabata
gabata@med.kanazawa-u.ac.jp

[1] Department of Radiology, Graduate School of Medical Sciences, Kanazawa University, 13-1 Takaramachi, Kanazawa City, Ishikawa 920-8640, Japan

[2] Proton Therapy Center, Fukui Prefectural Hospital, Fukui 910-8526, Japan

characteristics of a Bragg peak, especially a spread-out Bragg peak. Particle beam therapy and SBRT are more useful than conventional RT because it is possible to improve the dose concentration to the patient's tumor and reduce the dose to the surrounding liver tissue, especially in large liver tumors [7, 8]. However, because of the physical characteristics of particle beam therapy and SBRT, this type of RT is easily affected by only small motion of the target. This is a weakness of particle beam therapy and SBRT. Therefore, highly accurate and reproducible irradiation is needed, which requires an understanding of how the target of irradiation moves.

In RT for abdominal organs, it is important to consider the respiratory motion. This is especially true for organs located at the vicinity of the diaphragm, such as the liver, which is highly mobile during respiration [9–11]. Various devices and techniques have been used in an attempt to reduce the internal margin, such as abdominal compression [12], the self-breath-holding technique [13, 14], use of an active breathing control system [15], respiration-gated stereotactic RT [16–18], and tumor-tracking RT with fiducial markers [19].

The recurrence rate of liver cancer is rather high; thus, multidisciplinary treatments combining surgery, chemical treatment, transcatheter arterial embolization, radiofrequency ablation, and RT are becoming increasingly more important.

Abdominal surgery reduces the intestinal motor function because of gastrointestinal adhesion formation, sometimes resulting in intestinal obstruction [20–24]. We hypothesized that these adhesions might also reduce the respiratory liver motion. Therefore, the respiratory motion of the liver might be different with versus without surgery, necessitating consideration of the optimal margin of internal motion in radiation treatment planning.

In modern RT, four-dimensional computed tomography (4D-CT) has become a standard technique with which to evaluate the internal margin of target volumes, and it is reportedly a useful tool for analysis of the dynamic respiratory motion of various organs [25–28].

Several reports have analyzed the respiratory motion of the liver using this technique; however, few have analyzed the respiratory motion in each segment of the liver, and it is therefore difficult to understand the differences among the segments. Additionally, no reports have evaluated the influence of tissue adhesion caused by abdominal surgery on respiratory motion.

Therefore, in the present study, patients were grouped according to liver segment and history of abdominal (hepatobiliary/pancreatic) surgery, and their respiratory motion was analyzed and statistically compared.

Materials and methods

Patients and data acquisition

This retrospective study was approved by the research ethics committee of our institution (IRB number: 12–10), and written informed consent for this study was waived because of its retrospective nature. From March 2011 to July 2013, patients who were treated using proton beam therapy for abdominal cancer were enrolled. Patients were not eligible for this study if they could not control a stable respiratory rhythm suitable for 4D-CT scan conditions.

The patients were placed in the supine position and immobilized using a vacuum lock bag and a low-temperature thermoplastic body shell (ESFORM; Engineering System Co., Nagano, Japan). We did not control the amount of motion due to abdominal compression.

Respiratory synchronized 4D-CT (Aquilion LB; Toshiba Medical Systems Co., Tochigi, Japan) was performed under the following conditions: X-ray tube voltage, 120 kV; tube current, 200–300 mA; and rotation time, 500 ms. The 4D helical scan was performed using breathing synchronization. Respiratory gating was controlled by abdominal wall motion with the laser sensor of a respiratory gating system (AZ-733 V; Anzai Medical Co., Tokyo, Japan). The patient was asked to perform stable breathing with a respiratory frequency of 10–12 breaths/min by following a metronome. The up–down motion of the abdominal skin surface was detected in real time by a non-contact type sensor equipped in the respiratory synchronization system, and the respiratory wave signal generated by the system was used to monitor the patient's respiratory status. The wave signal was transferred to the 4D-CT scanner, allowing for reconstruction of a set of CT images associated with any of the respiratory phases. The reconstruction conditions of the CT images were as follows: slice thickness, 2 mm and slice interval, 0.4 mm; the field of view was set to match the physique of the patient.

Data analysis

In this study, we analyzed 4D-CT data acquired for the planning of proton beam therapy. Based on these images, the respiratory motion of a high-density lesion and iatrogenic metal (evaluation point) in the liver parenchyma were analyzed as position indicators by a radiation oncologist and a radiation technologist with more than 10 years of experience in RT. For high-density lesions, we targeted areas of calcification and Lipiodol remaining within the vessel in cases of enforcement by hepatic arterial

embolization. In surgical patients, we also targeted surgical metal implants (staplers and stents) (Fig. 1).

The evaluation points were grouped based on the Couinaud liver segment classification. We then measured the amount of motion of each liver segment in each respiratory phase. Based on the respiratory wave signal, one respiratory cycle was separated into eight phases: the end of the inspiration phase, corresponding to the maximum amplitude of the wave signal (No. 0); three equally divided phases from the end of inspiration to the end of expiration (Nos. 1–3); the end of the expiration phase, corresponding to the minimum amplitude of the wave signal (No. 4); and three equally divided phases from the end of expiration to the end of inspiration (Nos. 5–7). The respiratory motion of the liver and diaphragm in all eight phases was measured along the three orthogonal axes. The *x*-, *y*-, and *z*-axes correspond to the lateral (right–left), vertical (anterior–posterior), and long (inferior–superior) directions, respectively.

The positions of these evaluation points in each respiratory phase from No. 0 to 7 were measured in the CT images as shown in Fig. 2a. The motion of all evaluation points in each respiratory phase was evaluated by the relative position referenced to the end of expiration phase (No. 4). This is because during respiratory gated proton beam therapy, the gated irradiation was generally performed within the threshold at the end of the expiration phase, where the motion was considered to be more stable than in the other phases; thus, we defined the position in phase No. 4 as the reference for the motion analysis.

Next, as shown in Fig. 2b, we created a waveform showing the amount of respiratory motion. Using the coordinates of the eight phases, we drew this waveform as a smooth, continuous curve for interpolating the discrete

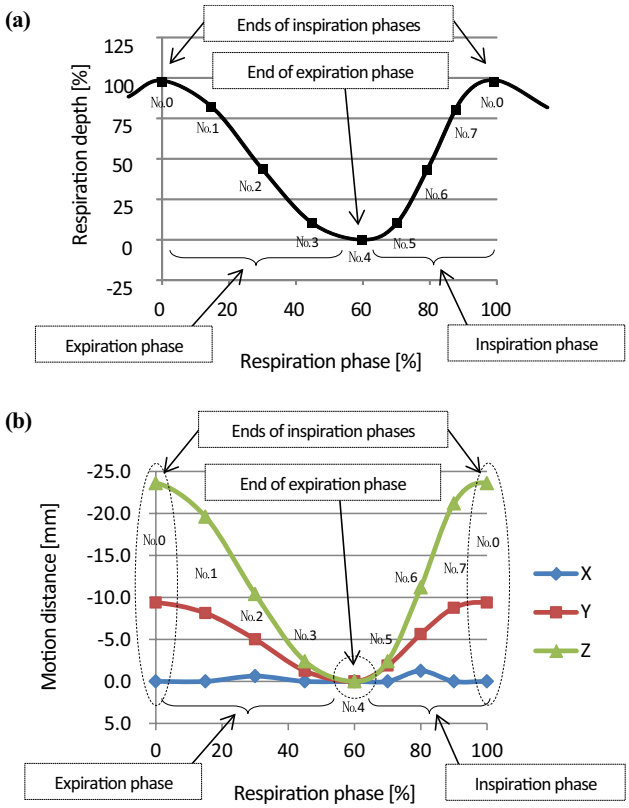

Fig. 2 **a** Respiratory waveform. The vertical axis represents the depth of respiration. 0 and 100% in the horizontal axis correspond to the end of one inspiration phase and the end of the next inspiration phase, respectively. **b** Respiratory motion. The vertical axis shows the respiratory motion. The horizontal axis is identical to that in **a**. In the legend, the curves of *X*, *Y*, and *Z* indicate the lateral, vertical and long direction of the patient, respectively

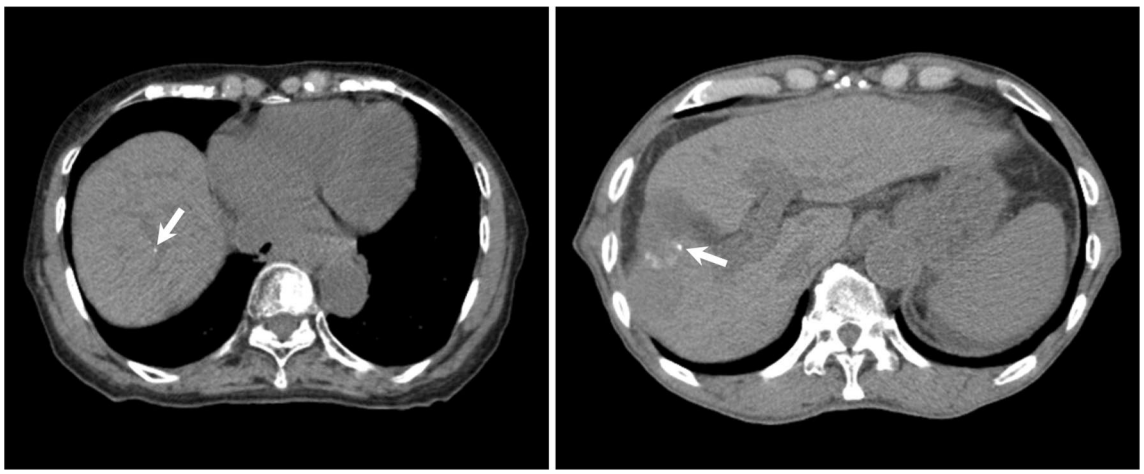

Fig. 1 Examples of evaluation points in CT images. Left: calcification, right: Lipiodol

points based on the function of the cubic spline curve [29, 30].

For all evaluation points, the motion distance between the end of the inspiration phase and the end of the expiration phase was calculated. These evaluation points were grouped according to the presence or absence of a history of abdominal surgery and according to the liver segment, and the differences in the respiratory motion of each group were compared.

Comparisons between two independent groups were analyzed using Mann–Whitney *U* test (hereinafter, *U* test). A p value of < 0.05 was considered statistically significant. Statistical analyses were performed using software (SPSS Version 23; IBM, Armonk, NY).

Results

The respiratory motion at the 218 evaluation points in 57 patients who underwent proton beam therapy was analyzed. The patient characteristics and evaluation points (numbers of patients with and without a history of abdominal surgery grouped by liver segment, etc.) are shown in Table 1. Fasting for > 3 hours before CT was performed in all cases. No patients had a protruding type hepatocellular carcinoma. The patients' motion trajectories are shown in Fig. 3, and the amounts of motion are shown in Table 2. Figure 3 depicts the trajectory of one respiration cycle with the evaluation point positioned at the end of the expiratory phase as the origin. One evaluation point is one loop curve.

Figure 3 confirms that the trajectory of respiratory motion varied considerably among the liver segments in both patients with and without a history of abdominal surgery. In each segment, the motion relative to the end of the inspiration phase with reference to the end of the expiration phase exhibited a trajectory toward the inferior direction and anterior direction of the trunk. Additionally, the respiratory motion generally tended to be smaller in patients with than without a history of abdominal surgery.

As shown in Table 2, the median (range) respiratory motion of the liver as a whole in patients without a history of surgery was 19.1 (2.5–59.7) mm, but the minimum was 15.1 (10.6 –19.3) mm in S4 and the maximum was 29.0 (7.2–42.1) mm in S6. Table 3 shows that the amount of motion of the right lobe and caudate lobe was large, whereas the motion of the left lobe was small.

Among patients with a history of abdominal surgery, the amount of motion of the whole liver was 12.0 (3.7–47.3) mm; in terms of segment, the minimum was 6.3 (4.1–9.3) mm in S3 and the maximum was 28.0 (9.0–37.4) mm in S7. The amount of motion of the right lobe was large, whereas the amount of motion of the left lobe and caudate lobe was small.

Table 1 Patient characteristics and evaluation points

Characteristics	
Age in years	Median, 70 (range 40–86)
Sex, male/female	33/24
Cirrhosis, no/yes	14/43
Site of proton beam therapy	
Liver	50
Bile duct	4
Pancreas	1
Abdominal lymph node	2
History of abdominal surgery, no/yes	39/18
Site of surgery[a]	
Liver	10
Gall bladder	8
Bile duct	2
Pancreas	4
Surgical method	
Skin incision	15
Laparoscopic approach	3
History of other pretreatment[a]	
RFA	14
TACE	23
TAE	4
PEIT	2
Numbers of evaluation points, no/yes	
S1	11/12
S2	8/12
S3	6/10
S4	6/12
S5	12/9
S6	11/8
S7	11/7
S8	18/8
Diaphragm	39/18

RFA radiofrequency ablation, *TACE* transcatheter arterial chemoembolization, *TAE* transcatheter arterial embolization, *PEIT* percutaneous ethanol injection therapy

[a]The site of surgery and history of other pretreatment included overlapping cases

Comparison of the amount of motion in patients with and without a history of abdominal surgery showed a commonality in that the right lobe was large and the left lobe was small; however, the opposite tendency was shown for the caudate lobe (Table 3). Among the segments of the right lobe with large motion, the posterior segments (S6 and S7) moved more than the anterior segments (S5 and S8). S6 and S7, which are located far from the lung and diaphragm, moved more than S8, which is the most closely adjacent to the diaphragm.

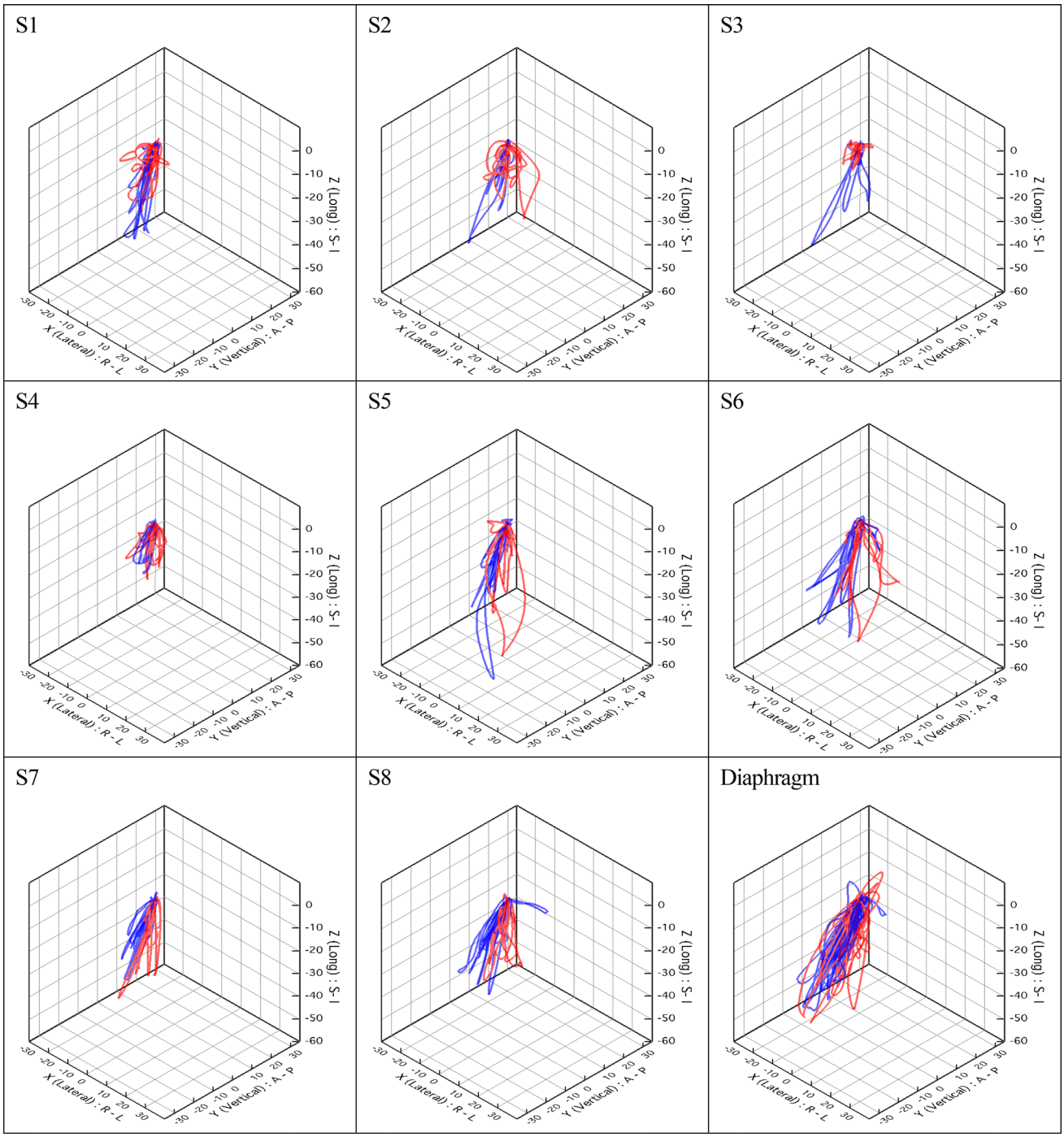

Fig. 3 Motion trajectory of evaluation points in each liver segment (unit: mm). Each looped curve depicts the trajectory during one respiration cycle in one patient. The red and blue curves show the trajectory in patients with and without a history of abdominal surgery, respectively (color figure in online version only)

When we compared the results of this study with the report describing the abdominal compression method [12, 31, 32], the effect of suppressing diaphragm motion was smaller in our patients with a history of surgery than in patients who underwent the abdominal compression method as the auxiliary treatment technique in previous studies.

When the change in the amount of motion in patients with versus without a history of surgery was analyzed by the *U* test, $p = 0.001$ was obtained for the whole liver, indicating a significant difference. Assessment of S3 revealed a p value of 0.007, showing a significant difference; there were no significant differences in the other segments (Table 2).

Table 2 Median, minimum, and maximum motion distances among patients with and without a history of abdominal surgery

Position	Surgery (−)		Surgery (+)		*p* value
	Median	Range	Median	Range	
S1–S8 total	19.1	2.5–59.7	12.0	3.7–47.3	0.001
S1	22.0	4.6–34.9	10.9	4.9–24.2	0.074
S2	17.1	2.5–39.0	11.9	4.5–25.2	0.316
S3	16.6	8.1–45.7	6.3	4.1–9.3	0.007
S4	15.1	10.6–19.3	11.6	3.8–21.5	0.349
S5	17.9	5.0–59.7	12.2	5.9–47.3	0.670
S6	29.0	7.2–42.1	26.2	3.7–41.8	0.563
S7	20.7	16.1–33.2	28.0	9.0–37.4	0.821
S8	20.2	13.0–39.3	24.4	11.8–42.5	1.000
Diaphragm	26.0	9.1–45.3	23.5	5.1–48.2	0.797

The motion distances are presented in millimeters and are shown for the whole liver as well as each individual segment. The far right *p* values compared the median values between patients with and without a history of surgery in each segment (*U* test analysis)

Table 3 Relative magnitude of respiratory motion in each liver segment

Surgery	Magnitude
(−)	S4 < S3 < S2 < S5 < S8 < S7 < S1 < S6
(+)	S3 < S1 < S4 < S2 < S5 < S8 < S6 < S7

As shown in Fig. 3, only one patient among those without a history of surgery showed a unique trajectory of S8. In this patient, the motion of S8 was compared with that of S5, S7, and the diaphragm apex; a similar tendency was also shown at the diaphragm apex, whereas S5 and S7 had no specificity.

Discussion

In this study, we analyzed the influence of abdominal surgery on respiratory liver motion by 4D-CT. No previous reports have analyzed the changes in liver motion after abdominal surgery.

The liver contains various ligaments (hepatoduodenal ligament, coronary ligament, and falciform ligament) that extend from its surface to the diaphragm and anterior abdominal wall. These ligaments are folds of peritoneum that anchor the liver into place. These ligaments and surrounding structures (e.g., inferior vena cava, diaphragm) might affect the respiratory liver motion.

In the comparison of the amount of motion of each liver segment, the right lobe showed a large amount of motion and the left lobe showed a small amount of motion regardless of the presence of a history of abdominal surgery. We speculate that the low degree of freedom of motion was caused by the presence of the heart, stomach, and colon around the left lobe. These results suggest that the internal margin could be reduced in the left lobe.

Among the segments in the right lobe with a large amount of motion, the posterior segments (S6 and S7) moved more than the anterior segments (S5 and S8). However, S6 and S7, which are located far from the lung and diaphragm, moved more than S8, the most adjacent segment to the diaphragm. In each segment, the motion relative to the end of the inspiration phase with reference to the end of the expiration phase exhibited a trajectory toward the inferior direction and anterior direction of the trunk (Fig. 3). The lower lung lobes (S9 and S10) are located on the upper back side of the liver, and we deduce that they push the liver toward the inferior and anterior direction. Nishioka et al. [33] reported the direction of motion with a vector in only one direction (toward the diaphragm), and our results do not contradict these motion analysis results using gold markers in the liver. Additionally, when comparing the trajectory from the end of the inspiration phase to the end of the expiration phase versus the trajectory from the end of the expiration phase to the end of the inspiration phase, we found that they moved in different routes. This tendency was particularly strong in patients with a history of surgery, and the variation of the route increased in each of these patients.

Table 2 shows that in each segment other than S7/8, respiratory motion was smaller in patients with than without a surgical history. This may have been because postoperative tissue adhesion decreases the mobility of the liver. Analysis of the amount of motion in each segment showed smaller differences among the segments in patients without a surgical history and larger differences in patients with a surgical history. This result might be explained by the fact that part of the liver is fixed in the abdominal cavity by tissue adhesion, and the degree of freedom of the unfixed segment may be relatively increased. Additionally, the surgical site differs for each patient, and this variation might have affected the result. We consider that the more movable part of the liver after surgery is not clinically preferred. Therefore, close attention should be given to postoperative changes in liver mobility.

As shown in Fig. 3, only one patient among those without a history of abdominal surgery showed unique motion in the trajectory of S8 and the diaphragm apex. In this patient, the pleural effusion was stored in the lung field, and we considered that this suppressed the motion of the diaphragm and S8 toward the superior–inferior direction immediately below the pleural effusion. The distance from the pleural effusion to S5 and S7 is greater than that to S8;

therefore, the influence was considered relatively small and did not considerably change the trajectory. Based on the above findings, there is a possibility that the motion of the liver shows a different trend between patients with and without pleural effusion, and special care should thus be taken in setting the irradiation field for patients with pleural effusion.

The present study had several limitations. First, 4D-CT images could not be acquired for the patients with an irregular respiratory cycle, and the respiratory motion with an irregular respiratory rhythm could not be analyzed. Second, the group of patients with a history of abdominal surgery included both patients who underwent hepatobiliary surgery and those who underwent pancreatic surgery. The differences in the organs involved in these operations (liver, bile duct, and pancreas) might have affected the liver motion. Besides surgery, a history of radiofrequency ablation, transcatheter arterial chemoembolization, transcatheter arterial embolization, and percutaneous ethanol injection therapy may also have effects. Third, although the evaluation point is in the same segment, its position varies from case to case; it is not necessarily at the center of gravity of the segment, and it is considered to contain potential errors. Fourth, the conditions of the thorax affect the liver motions with respect to the presence or absence of pleural effusion. In further studies, patient groups should be classified according to more details of the operation site and thorax conditions. However, our data show the detailed respiratory motion of the liver. These findings suggest that when performing RT of the liver, it is necessary to selectively use the internal margin setting depending on the segment to be irradiated and the patient's history of abdominal surgery.

Conclusions

Analysis using 4D-CT confirmed the detailed respiratory motion of the liver. The distances and directions of the respiratory motion differed for each liver segment, and a history of abdominal surgery reduced the respiratory motion of the liver. These findings suggest that when performing RT of the liver, it is necessary to selectively use the internal margin setting depending on the segment to be irradiated and the patient's history of abdominal surgery.

Acknowledgements We gratefully acknowledge the work of the members of the Proton Therapy Center at Fukui Prefectural Hospital as well as the staff of the Radiology Department at Kanazawa University for their understanding and support.

Funding This research did not receive any specific grant from funding agencies in the public, commercial, or not-for-profit sectors.

Compliance with ethical standards

Conflicts of interest We declare no actual or potential conflicts of interest.

Ethical statement This retrospective study was approved by the research ethics committee of our institution.

References

1. World Health Organization. World Cancer Report 2014. pp. 403-412 Chapter 5.6. ISBN 9283204298. http://publications.iarc.fr/Non-Series-Publications/World-Cancer-Reports/World-Cancer-Report-2014 Accessed August 1, 2017.
2. World Health Organization. World Cancer Report 2014. pp. 16-53 Chapter 1.1. ISBN 9283204298. http://publications.iarc.fr/Non-Series-Publications/World-Cancer-Reports/World-Cancer-Report-2014 Accessed August 1, 2017.
3. Takeda A, Sanuki N, Tsurugai Y, Iwabuchi S, Matsunaga K, Ebinuma H, et al. Phase 2 study of stereotactic body radiotherapy and optional transarterial chemoembolization for solitary hepatocellular carcinoma not amenable to resection and radiofrequency ablation. Cancer. 2016;122:2041–9. https://doi.org/10.1002/cncr.30008.
4. Takeda A, Sanuki N, Tsurugai Y, Oku Y, Aoki Y. Stereotactic body radiotherapy for patients with oligometastases from colorectal cancer: risk-adapted dose prescription with a maximum dose of 83–100 Gy in five fractions. J Radiat Res. 2016;57:400–5. https://doi.org/10.1093/jrr/rrw029.
5. Mizumoto M, Okumura T, Hashimoto T, Fukuda K, Oshiro Y, Fukumitsu N, et al. Proton beam therapy for hepatocellular carcinoma: a comparison of three treatment protocols. Int J Radiat Oncol Biol Phys. 2011;81:1039–45. https://doi.org/10.1016/j.ijrobp.2010.07.015.
6. Komatsu S, Fukumoto T, Demizu Y, Miyawaki D, Terashima K, Sasaki R, et al. Clinical results and risk factors of proton and carbon ion therapy for hepatocellular carcinoma. Cancer. 2011;117:4890–904. https://doi.org/10.1002/cncr.26134.
7. Suit H, Goldberg S, Niemierko A, Trofimov A, Adams J, Paganetti H, et al. Proton beams to replace photon beams in radical dose treatments. Acta Oncol. 2003;42:800–8. https://doi.org/10.1080/02841860310017676.
8. Coutrakon G, Bauman M, Lesyna D, Miller D, Nusbaum J, Slater J, et al. A prototype beam delivery system for the proton medical accelerator at Loma Linda. Med Phys. 1991;18:1093–9. https://doi.org/10.1118/1.596617.
9. Kirilova A, Lockwood G, Choi P, Bana N, Haider MA, Brock KK, et al. Three-dimensional motion of liver tumors using cine-magnetic resonance imaging. Int J Radiat Oncol Biol Phys. 2008;71:1189–95. https://doi.org/10.1016/j.ijrobp.2007.11.026.
10. Akino Y, Oh RJ, Masai N, Shiomi H, Inoue T. Evaluation of potential internal target volume of liver tumors using cine-MRI. Med Phys. 2014;41:111704. https://doi.org/10.1118/1.4896821.
11. Park JC, Kim JS, Park SH, Webster MJ, Lee S, Song WY, et al. Four dimensional digital tomosynthesis using on-board imager for the verification of respiratory motion. PLoS One. 2014;9:e115795. https://doi.org/10.1371/journal.pone.0115795.
12. Lee S, Yang DS, Choi MS, Kim CY. Development of respiratory motion reduction device system (RMRDs) for radiotherapy in moving tumors. Jpn J Clin Oncol. 2004;34:686–91. https://doi.org/10.1093/jjco/hyh125.
13. Onishi H, Kuriyama K, Komiyama T, Tanaka S, Ueki J, Sano N, et al. CT evaluation of patient deep inspiration

self-breath-holding: how precisely can patients reproduce the tumor position in the absence of respiratory monitoring devices? Med Phys. 2003;30:1183–7. https://doi.org/10.1118/1.1570372.
14. Takamatsu S, Takanaka T, Kumano T, Mizuno E, Shibata S, Ohashi S, et al. Reproducibility of diaphragm position assessed with a voluntary breath-holding device. Jpn J Radiol. 2013;31:357–63. https://doi.org/10.1007/s11604-013-0199-3.
15. Dawson LA, Eccles C, Bissonnette JP, Brock KK. Accuracy of daily image guidance for hypofractionated liver radiotherapy with active breathing control. Int J Radiat Oncol Biol Phys. 2005;62:1247–52. https://doi.org/10.1016/j.ijrobp.2005.03.072.
16. Underberg RW, Lagerwaard FJ, Slotman BJ, Cuijpers JP, Senan S. Benefit of respiration-gated stereotactic radiotherapy for stage I lung cancer: an analysis of 4DCT datasets. Int J Radiat Oncol Biol Phys. 2005;62:554–60. https://doi.org/10.1016/j.ijrobp.2005.01.032.
17. Ohara K, Okumura T, Akisada M, Inada T, Mori T, Yokota H, et al. Irradiation synchronized with respiration gate. Int J Radiat Oncol Biol Phys. 1989;17:853–7. https://doi.org/10.1016/0360-3016(89)90078-3.
18. Tsunashima Y, Vedam S, Dong L, Umezawa M, Sakae T, Bues M, et al. Efficiency of respiratory-gated delivery of synchrotron-based pulsed proton irradiation. Phys Med Biol. 2008;53:1947–59. https://doi.org/10.1088/0031-9155/53/7/010.
19. Shirato H, Shimizu S, Kunieda T, Kitamura K, van Herk M, Kagei K, et al. Physical aspects of a real-time tumor-tracking system for gated radiotherapy. Int J Radiat Oncol Biol Phys. 2000;48:1187–95. https://doi.org/10.1016/S0360-3016(00)00748-3.
20. Weibel MA, Maino G. Peritoneal adhesions and their relation to abdominal surgery. A postmortem study. Am J Surg. 1973;126:345–53. https://doi.org/10.1016/S0002-9610(73)80123-0.
21. ten Broek RP, Issa Y, van Santbrink EJ, Bouvy ND, Kruitwagen RF, Jeekel J, et al. Burden of adhesions in abdominal and pelvic surgery: systematic review and met-analysis. BMJ. 2013;347:f5588. https://doi.org/10.1136/bmj.f5588.
22. Quatromoni JC, Rosoff L, Halls JM, Yellin AE. Early postoperative small bowel obstruction. Ann Surg. 1980;191:72–74. https://www.ncbi.nlm.nih.gov/pmc/articles/PMC1344621/pdf/annsurg00227-0086.pdf. Accessed August 1, 2017.
23. Menzies D, Elis H. Intestinal obstruction from adhesions–how big is the problem? Ann R Coll Surg Engl. 1990;72:60–63. https://www.ncbi.nlm.nih.gov/pmc/articles/PMC2499092/pdf/annrcse01560-0064.pdf. Accessed August 1, 2017.
24. ten Broek RP, Stommel MW, Strik C, van Laarhoven CJ, Keus F, van Goor H. Benefits and harms of adhesion barriers for abdominal surgery: a systematic review and meta-analysis. Lancet. 2014;383:48–59. https://doi.org/10.1016/S0140-6736(13)61687-6.
25. Hallman JL, Mori S, Sharp GC, Lu HM, Hong TS, Chen GT. A four-dimensional computed tomography analysis of multiorgan abdominal motion. Int J Radiat Oncol Biol Phys. 2012;83:435–41. https://doi.org/10.1016/j.ijrobp.2011.06.1970.
26. Kumagai M, Mori S. Movement of a small tumour in contact with the diaphragm: characterisation with four-dimensional CT. Jpn J Radiol. 2016;34:154–7. https://doi.org/10.1007/s11604-015-0509-z.
27. Fernandes AT, Apisarnthanarax S, Yin L, Zou W, Rosen M, Plastaras JP, et al. Comparative assessment of liver tumor motion using cine-magnetic resonance imaging versus 4-dimensional computed tomography. Int J Radiat Oncol Biol Phys. 2015;91:1034–40. https://doi.org/10.1016/j.ijrobp.2014.12.048.
28. Gabryś D, Kulik R, Trela K, Ślosarek K. Dosimetric comparison of liver tumour radiotherapy in all respiratory phases and in one phase using 4DCT. Radiother Oncol. 2011;100:360–4. https://doi.org/10.1016/j.radonc.2011.09.006.
29. Liu Y, Jin R, Chen M, Song E, Xu X, Zhang S, et al. Contour propagation using non-uniform cubic B-splines for lung tumor delineation in 4D-CT. Int J Comput Assist Radiol Surg. 2016;11:2139–51. https://doi.org/10.1007/s11548-016-1457-5.
30. Feng Z, Li A, Gong H, Luo Q. An automatic method for nucleus boundary segmentation based on a closed cubic spline. Front Neuroinform. 2016;10:21. https://doi.org/10.3389/fninf.2016.00021.
31. Eccles CL, Patel R, Simeonov AK, Lockwood G, Haider M, Dawson LA. Comparison of liver tumor motion with and without abdominal compression using cine-magnetic resonance imaging. Int J Radiat Oncol Biol Phys. 2011;79:602–8. https://doi.org/10.1016/j.ijrobp.2010.04.028.
32. Hu Y, Zhou YK, Chen YX, Shi SM, Zeng ZC. 4D-CT scans reveal reduced magnitude of respiratory liver motion achieved by different abdominal compression plate positions in patients with intrahepatic tumors undergoing helical tomotherapy. Med Phys. 2016;43:4335. https://doi.org/10.1118/1.4953190.
33. Nishioka T, Nishioka S, Kawahara M, Tanaka S, Shirato H, Nishi K, et al. Synchronous monitoring of external/internal respiratory motion: validity of respiration-gated radiotherapy for liver tumors. Jpn J Radiol. 2009;27:285–9. https://doi.org/10.1007/s11604-009-0332-5.